

Radiation Effects in MicroElectroMechanical Systems (MEMS): RF Relays

S. McClure, L. Edmonds, R. Mihailovich, A. Johnston, *Fellow, IEEE*, P. Alonzo, J. DeNatale, *Member, IEEE*, J. Lehman, C. Yui

Abstract—GaAs Microelectromechanical RF relays fabricated by surface micromachining techniques were characterized for their response to total ionizing dose. Micro relays with two different geometries were studied. For one geometry, changes in switch actuation voltage at moderate dose levels were observed. For an alternate geometry no change in actuation voltage was observed. A mechanism for dielectric charge trapping and its effect on the electrostatic force is proposed.

I. INTRODUCTION

Microelectromechanical systems (MEMS) are receiving increasing interest for use in space systems. One particular area of interest is in Picosats [1,2], 1-kg class satellites, where very little shielding is afforded to the space radiation environment. To date, however, few radiation tests have been performed on MEMS devices. Tests performed by the Naval Research Laboratory and the Jet Propulsion Laboratory on MEMS accelerometers have shown the technology prone to radiation effects at moderate dose levels [3,4]. On the other hand, tests performed by Sandia National Laboratories on surface micromachined comb drives and microengines [5] indicated that total dose had an effect only at very high dose levels, ~10 Mrd. In all cases, the observed radiation effects were attributed to electrostatic force caused by charge accumulation in SiO_2 and Si_3N_4 dielectric layers. A quantitative model for this electrostatic force was developed for some mechanical structures by Edmonds [6].

In this study, the electrical performance of MEMS RF relays (switches) is evaluated in the gamma total dose environment. Switches of this type are of interest due to their very low insertion loss for RF/microwave signals, low power consumption, small size/weight, and their compatibility with monolithic integration with active circuitry. Such devices

offer attractive performance benefits in a broad range of communications and radar applications, such as tunable/switchable filters, low-loss signal routing networks, dynamic band selection, and phase shifter circuits for electronically scanned antennas. The devices in this study included two different configurations of RF MEMS switches from Rockwell Scientific Company, each utilizing a different geometry for the electrostatic actuator. One geometry consists of a dielectric layer between the actuator plates (“standard” configuration), while the other had the dielectric layer above the upper actuator plate (an “alternate” configuration). The dielectric layer for both configurations of this device was a proprietary amorphous material that was the same material for both designs. A similar device, manufactured by HRL Laboratories, Malibu, California, with a dielectric layer identified as Si_xN_y between the actuator plates was previously tested with no observed radiation effects to 1 Mrd [7]. In that study, the device was operated dynamically. In the present study, radiation effects were observed at much lower dose levels with the devices operated statically.

II. DEVICE DESCRIPTIONS

The devices obtained for this study from Rockwell Scientific Company (RSC) were engineering development samples produced and packaged for this test. The RSC relay is fabricated by surface micromachining techniques, using low-temperature <250C thin films deposited atop the GaAs substrate. Details of the fabrication process are described elsewhere [8], and the process will only be summarized here. First, signal lines found on the substrate are defined by lift-off patterning of evaporated Au films. A sacrificial layer is then formed from a spun and planarized organic layer. This sacrificial layer serves as a platform, that is eventually removed, for building the relay mechanical structure. Windows etched in this organic define the anchor regions for the mechanical structure. The electrical shunting bar is defined atop the sacrificial layer by lift-off patterning of evaporated gold. Next, the mechanical structure is constructed from PECVD dielectric film deposition of the structural layer, lift-off of the drive metal patterns, and etching of the PECVD film. The entire relay microstructure is made freestanding in the final fabrication step by isotropic

This work was carried out at the Jet Propulsion Laboratory, California Institute of Technology, under contract with the National Aeronautics and Space Administration, Code AE, under the NASA Electronics Parts and Packaging Program (NEPP). Additional support was provided by Rockwell Scientific Corporation, Thousand Oaks, CA.

Steven S. McClure, L. Edmonds, A. Johnston, J. Lehman, C. Yui and P. Alonzo are with the Jet Propulsion Laboratory, Pasadena, CA 91109 USA (telephone: 818-354-0482, e-mail: steven.s.mcclure@jpl.nasa.).

R. Mihailovich and J. DeNatale are with Rockwell Scientific Company, Thousand Oaks, CA 91360 USA (telephone: 805-373-4841, e-mail: rmihailovich@rWSC.com).

O_2 dry etching of the sacrificial organic layer. The specific composition of the structural dielectric layer is proprietary.

For this evaluation, devices with the two different actuator configurations were fabricated on the same wafer. Switch topology and vertical cross sections are illustrated schematically in Figs. 1 and 2 respectively. As shown in Fig. 2, the primary difference between the two configurations, termed ‘standard’ and ‘alternate’, was the location of the dielectric with respect to the drive capacitor plates. For the standard configuration, the dielectric is between the plates, while for the alternate case it is above the upper plate. In both cases, the approximate dimensions of the drive capacitor plates are 100 by 100 μm and the thickness of the dielectric is 2 μm . The device is operated by applying voltage across the top and bottom drive capacitor plates producing the attractive electrostatic force necessary to overcome the spring force and to bring the contact bridge in contact with the underlying RF line. This makes continuity across the signal line gap (Fig. 1), providing a low-loss transmission path for the RF signal. When the drive voltage is removed, the elastic energy in the mechanical flexures opens the switch, breaking contact and providing high electrical isolation between the input and output ports. The nominal switch operating voltage for the device was 60V with an approximate contact force at this voltage of 50 to 100 μN . The threshold mechanical actuation (i.e. pull-in) voltage for the devices tested was approximately 55V and 45V respectively for the standard and alternate configurations. For both configurations, the air gap between the moving structure and the bottom capacitor plate is approximately 3.5 μm while open and 0.8 μm when closed.

It should be noted that the alternate configuration of the device was developed by RSC primarily to reduce the effects of electrostatic charging of the dielectric for which devices of this type have been shown to be susceptible [9]. This modification resulted in no performance degradation. Overall electrical performance of the two configurations is nearly identical.

III. EXPERIMENTAL DETAILS

A. Irradiation Facilities

Total dose, gamma irradiations were performed at the ^{60}Co range source at the Jet Propulsion Laboratory, Pasadena, CA. Dose rate was 50 rd(GaAs)/s. This source is in compliance with MIL-STD-883, Method 1019, and the required PbAl shields were used in all exposures. Total dose was determined from the source calibration data and verified using an ionization chamber.

B. Electrical Tests

Electrical tests for all devices were performed in-situ and included the actuation voltage for the actuation electrodes (drive capacitor). Though the device is typically operated using a positive voltage (top electrode with respect to the

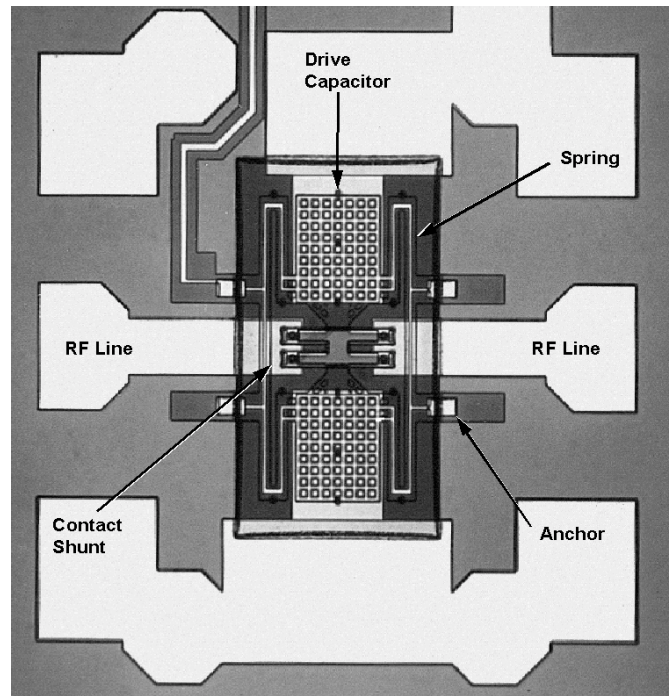


Fig. 1. Top view of the RSC MEMS RF switch. The center structure is suspended by the four metal springs. Application of voltage to the drive capacitor actuates the switch.

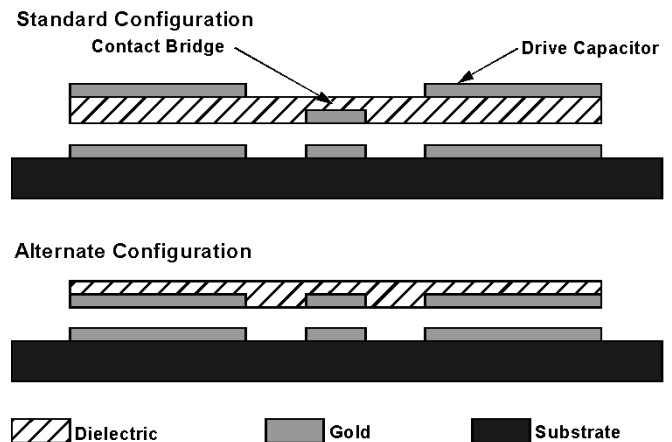


Fig. 2. Cross section of standard and alternate configurations of the RSC RF MEMS Switch.

substrate electrode), the device could be actuated in either positive or negative polarity. Taking advantage of this, the actuation voltage was tested in both polarities. Tests in the negative polarity were added as a diagnostic technique. The actuation voltage was simply determined by increasing the voltage to the drive capacitor slowly and observing the point at which the RF contacts went to low impedance as observed by applying 1 volt through 1 Kohm and observing the current through the contact.

C. Procedure

Test samples were irradiated one at a time and tested in step level fashion. Bias was maintained statically with the

device either in the “ON” or “OFF” state. Bias conditions and device configurations for each test are identified in Table I. One device of each type was tested in each of the positive and negative bias “ON” conditions. Though not the normal operational condition, tests of the negative bias case were performed as a diagnostic tool to evaluate the charging mechanism of the device. The “OFF” condition, 0V applied to the drive capacitor, was tested for the standard configuration after this configuration was found to exhibit radiation sensitivity in the biased conditions. In addition one device of the standard configuration was tested as an unirradiated control. In this case the device was simply maintained in the closed condition with +90V for two hours and the actuation voltage was tested. This was done since devices of this type are known to be prone to electrostatic charging from normal operation [9]. The control test would ensure that any true radiation induced effects would not be confused with this operation induced charging effect.

IV. TEST RESULTS

A. RSC RF Relay – Standard configuration

Gamma total dose test results for actuation voltage for the standard configuration RSC relay are shown in Figs. 3 and 4 for the positive and negative bias conditions respectively. Note that the bias voltage refers to the voltage applied during irradiation. The two polarities indicated by the two curves in each figure refer to actuation voltages measured at the end of each irradiation step. For the positively biased device, the actuation voltage increased steadily, in the positive direction, with increasing dose. The device exceeded the nominal device actuation voltage, 60V, before the 50 Krd level. Actuation voltage continued to increase through the highest level tested, 300 Krd. The test was terminated at this level since the bias voltage, +90V, was exceeded. In contrast, the actuation voltage for the negatively biased device shifted in the negative direction. For this case the degradation was more rapid with the bias voltage, -90V, being exceeded at approximately 150 Krd. The positively biased device was then tested after an unbiased anneal period with a slight recovery of about 3V after 3 days at 25C. After a further unbiased anneal at 125C for 24 hours the device had recovered fully. It is significant to note that for both bias cases, the negative and positive actuation voltages shift in the same direction by the same amount, i.e. they remain translations of each other, differing by twice the nominal pre-radiation actuation voltage.

The device irradiated while unbiased showed no measurable degradation with total dose. Although not shown here, the test was completed to 300 Krd. In addition, a control device tested after actuation at +90V showed less than 3 volts of threshold shift.

B. RSC RF Relay – Alternate configuration

No significant degradation was found for the alternate configuration for either bias condition to greater than 150 Krd

TABLE I
BIAS CONDITIONS TESTED

Device type	Bias	State	Comments
Standard	+ 90V	Closed	Typical “ON” condition
Standard	- 90V	Closed	Diagnostic test
Standard	0V	Open	Typical “OFF” condition
Alternate	+ 90V	Closed	Typical “ON” condition
Alternate	- 90V	Closed	Diagnostic test

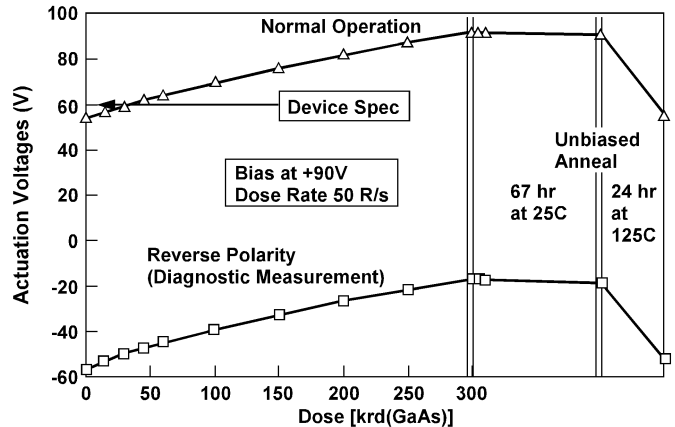


Fig. 3. Actuation voltage vs. dose for the standard configuration biased positively during irradiation.

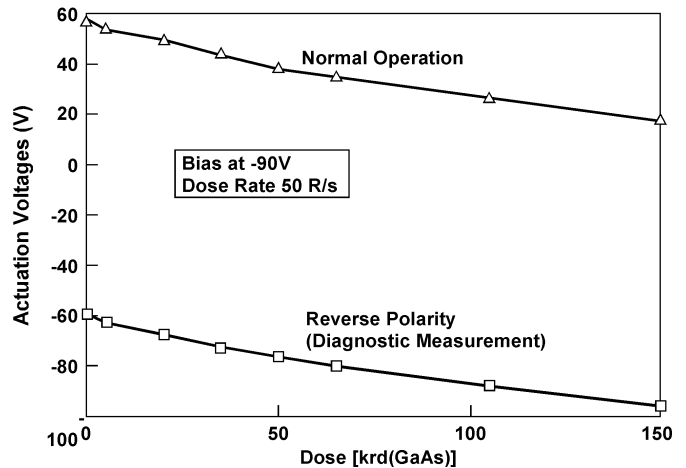


Fig. 4. Actuation voltage vs. dose for the standard configuration biased negatively during irradiation.

as indicated in Fig. 5 for the positive bias case. This is consistent with the results expected with the different location of the dielectric layer. In this case, the dielectric layer is above the top electrode. Charging within the dielectric in this location can have little effect on the actuation voltage of the switch.

V. MECHANISM

A. Theoretical prediction

Irradiation creates electron-hole pairs in the dielectric. In this amorphous dielectric, the electrons are fairly mobile and

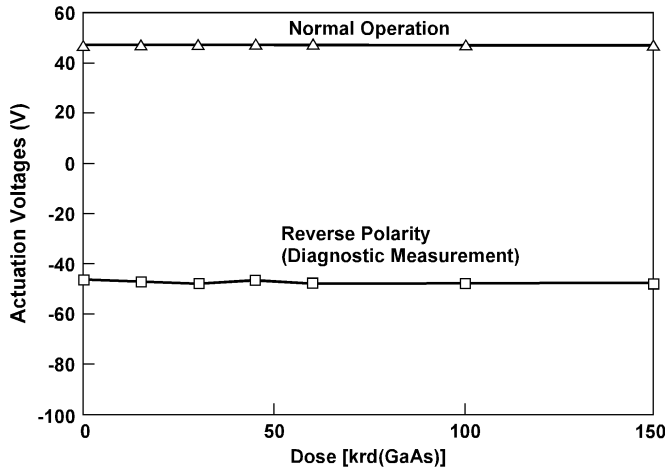


Fig. 5. Actuation voltage vs. dose for alternate configuration biased positively during irradiation. No measurable change in actuation voltage was observed.

the holes are semi-mobile, so carriers that survive the initial recombination can move in response to the electric field that is present in the dielectric during irradiation. Any carriers that become trapped after being displaced contribute to a semi-permanent charge distribution in the dielectric. There may also be a net dielectric charge via mechanisms suggested in the next section. Whether there is a net charge or merely a displacement of carriers (electrons in one direction and holes in the other) within the dielectric, the result is a charge distribution in the dielectric. This section regards the charge distribution as given and the objective is to theoretically predict the effect that this charge distribution has on the actuation voltage.

The physical arrangement is shown in Fig. 6. The dielectric thickness is T , the air gap thickness is L , and the area of the arrangement is A . The potential of the upper electrode relative to the lower electrode is V . The charge density (charge per unit volume) in the dielectric, denoted $\rho(z)$, is treated as uniform in the lateral dimensions so it is shown as a function of only the depth z . The dielectric is bonded to the upper electrode, so they are lumped together as a single system when calculating forces. This eliminates the need for including bonding forces in the analysis. The force that the lower electrode exerts on the upper system is the same as the force that the upper system exerts on the lower electrode. This electrostatic force can be calculated using the method in [6, appendix], which was derived for an arbitrary mechanical system, and the result is

$$F = \frac{A \epsilon_o \left[V + \frac{1}{\epsilon_r \epsilon_o} \int_0^T z \rho(z) dz \right]^2}{2 \left[\frac{T}{\epsilon_r} + L \right]^2} \quad (1)$$

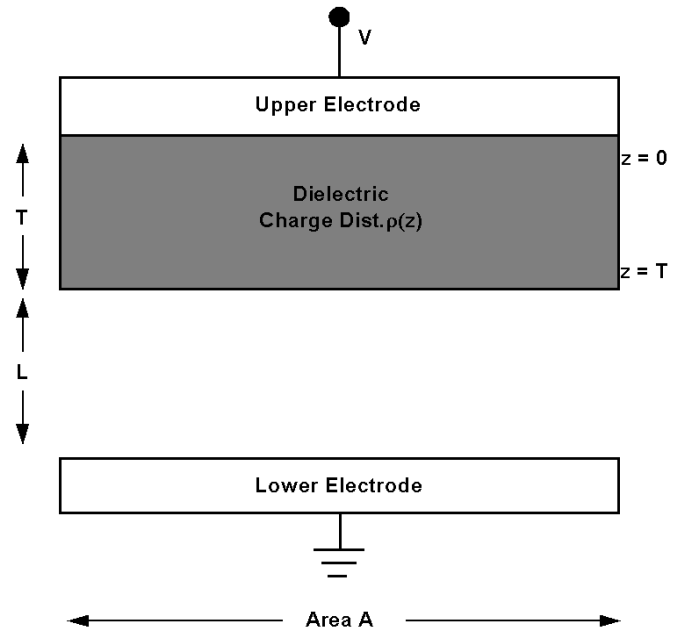


Fig. 6. Illustration for device charging mechanism calculation.

where F is the force, ϵ_r is the relative (dimensionless) dielectric constant of the dielectric, and ϵ_o is the free-space permittivity constant. The force is always (i.e., regardless of V or ρ) attractive, but the presence of a dielectric charge distribution can strengthen or weaken the force compared to the uncharged case at the same V . Note that the integral of ρ is weighted by the depth z , so charge near the bottom of the dielectric contributes more force than the same amount of charge near the top of the dielectric. Because of this weighting, a charge distribution can contribute to the force even if the net charge is zero, i.e., if carriers are moved within the dielectric but not removed from the dielectric.

It is seen from (1) that a voltage V_{irrad} applied to an irradiated dielectric will produce the same force as a voltage $V_{non-irrad}$ applied to a non-irradiated dielectric if the two voltages are related by

$$\left[V_{irrad} + \frac{1}{\epsilon_r \epsilon_o} \int_0^T z \rho(z) dz \right]^2 = [V_{non-irrad}]^2.$$

In particular, the actuation voltage for the irradiated case, denoted V_{act} , is related to the nominal (non-irradiated) actuation voltage, denoted $V_{nom-act}$, by

$$[V_{act} + \Delta V]^2 = [V_{nom-act}]^2 \quad (2)$$

where ΔV is defined by

$$\Delta V \equiv \frac{1}{\epsilon_r \epsilon_o} \int_0^z \rho(z) dz. \quad (3)$$

There are two solutions to (2) given by

$$V_{act} = -\Delta V - |V_{nom-act}| \quad (\text{one solution}) \quad (4a)$$

$$V_{act} = -\Delta V + |V_{nom-act}| \quad (\text{other solution}). \quad (4b)$$

The force equation (1) can be used to show that the switch is open (the force is too small to close it) if the applied voltage is between the two actuation voltages. Contact is made if the applied voltage is either larger (more positive or less negative) than the larger actuation voltage, or smaller (less positive or more negative) than the smaller actuation voltage. If there is no irradiation ($\Delta V = 0$), the two solutions are plus and minus the nominal actuation voltage. If irradiation produces a positive ΔV that increases with increasing dose, both actuation voltages decrease with dose (a positive voltage becomes less positive or a negative voltage becomes more negative). If irradiation produces a negative ΔV that becomes more negative with increasing dose, both actuation voltages increase (positive becomes more positive or negative becomes less negative). In either case, the strength (absolute value) of one actuation voltage increases while the other decreases. Stated another way, for a fixed dielectric charge distribution, the strength of the actuation voltage depends on whether the upper electrode is positive relative to the lower, or the lower is positive relative to the upper. The physical explanation for this distinction between up and down is that the dielectric is bonded to the upper electrode, so the electrostatic force between them is irrelevant, while the electrostatic force between dielectric and lower electrode is relevant. This is also the reason for the distinction between up and down that was stated earlier; that a charge low in the dielectric contributes more force than the same amount of charge high in the dielectric.

According to (4), there are two actuation voltages that implicitly depend on dose via ΔV . The difference between the two solutions is constant (equal to twice the nominal actuation voltage), so a plot of one solution versus dose is obtained by vertically translating a plot of the other solution. Experimental verification of this prediction was shown in Figs 3, 4 and 5.

B. Suggested charging mechanisms

The charge distribution in the dielectric produced by irradiation in the presence of a biasing voltage is complicated by the fact that, even when the switch is closed, there is an air gap between the dielectric and lower electrode. (The physical construction that produces this air gap is proprietary, so we are only at liberty to say that there is an air gap.) The system does not resemble a simple capacitor (a dielectric bonded between two electrodes) in which all liberated electrons that survive recombination are removed, leaving the surviving

holes behind to produce a net charge in the dielectric. In fact, a quantitative estimate of ΔV based on this capacitor model gives a predicted dose, corresponding to a given ΔV , that is orders of magnitude smaller than the experimentally observed dose. Dose has much less effect in the real device than in a hypothetical device described by these calculations, indicating that the charging mechanism is not the same as it is for a simple capacitor. However, some insight regarding the charge distribution might be obtained by combining the theory in the previous section with measured data. The agreement with data discussed at the end of the previous section suggests that the theory is correct, but it should still be acknowledged that we have no independent verification of the assertions below so they are offered here only as suggestions.

Negative Bias During Irradiation

Fig. 4 shows the case in which the upper electrode was negative relative to the lower electrode during irradiation. The actuation voltages decrease with dose, so ΔV in (4) is positive. The biasing during irradiation tends to displace holes upward and electrons downward within the dielectric. If the only charge motion were a displacement of carriers within the dielectric, then, according to (3), ΔV would be negative. Therefore there must be some other mechanism that causes the dielectric to become positively charged. The suggested mechanism is secondary electrons that are created low enough in the dielectric so that they are able to leave the dielectric before becoming thermalized. Any such electrons will be attracted (via the biasing voltage) to the lower electrode, so they do not return to the dielectric.

Positive Bias During Irradiation

Fig. 3 shows the case in which the upper electrode was positive relative to the lower electrode during irradiation. The figure shows that the actuation voltages increase with dose, so ΔV in (4) is negative. The biasing during irradiation tends to displace holes downward and electrons upward within the dielectric (the electrons might even be removed by the upper electrode). According to (3), this effect, by itself, would make ΔV positive. Therefore there must be some other mechanism that causes the dielectric (at least the bottom portion) to become negatively charged. The suggested mechanism is secondary electrons emitted from other device structures below the dielectric, e.g. the lower gold plate of the drive capacitor or the GaAs substrate. Such electrons will be attracted (via the biasing voltage) to the lower dielectric surface where they become trapped by surface states. Another contribution to this surface charge (perhaps significant and perhaps not) can come from secondary electrons emitted by the dielectric that then return to the dielectric surface via the biasing voltage. Moving negative charge lower in the dielectric (electrons formerly in the interior are moved to the lower surface) also contributes to a negative ΔV .

VI. DISCUSSION

It was theoretically predicted, and experimentally verified, that there are two actuation voltages for these switches. It was also theoretically predicted, and experimentally verified, that

the difference between these voltages is constant, i.e., a plot of one actuation voltage versus dose is obtained by vertically translating a plot of the other. The theory predicts actuation voltage when the dielectric charge distribution is given but does not predict the charge distribution as a function of irradiation history. However, some properties of the charging mechanisms were deduced by combining the theory with measured data. It appears that the charging mechanisms are very similar to those that were proposed earlier for a silicon-based MEMS accelerometer [6]. For the accelerometer, the polarity of the dielectric charge depends on two competing mechanisms: emission of secondary electrons from the dielectric, and emission of secondary electrons elsewhere in the device with some of these electrons adhering to the dielectric. For the accelerometer, the dominant mechanism depends on the type of irradiation (electron irradiation produced a different charge polarity than proton irradiation). A similar "contest" appears to apply to the switch device considered here, which is GaAs-based but contains proprietary dielectric capable of trapping charge. We did not investigate different irradiation sources for the switch device, but the dependence of charge polarity on biasing polarity (during irradiation) is consistent with the concept of these competing mechanisms. A voltage polarity that moves electrons away (down) from the dielectric produces a positive dielectric charge, while a voltage polarity that attracts electrons to the dielectric produces a negative dielectric charge.

There is another similarity between the GaAs-switch and the Si-accelerometer. While the polarity of the dielectric charge in the accelerometer was controlled by the two mechanisms discussed above, there is a third mechanism that influences the amount of charge. This is a leakage current in the dielectric via irradiation-induced conductivity (i.e., electron-hole pairs in the dielectric). This tends to discharge the dielectric; i.e. it competes with the dominant charging mechanism, so it limits the amount of charge that can be obtained. For the accelerometer, a limiting charge was seen as a saturation condition at large dose [6]. For the switch device considered here, the dose was not large enough to reach saturation, but the fact (or assertion) that leakage currents compete with the dominant charging mechanism is implied by the sign of ΔV . If the dielectric did not exchange charge with its environment, i.e., if the only charge motion was a displacement of carriers within the dielectric in response to the electric field, the polarity of ΔV would be opposite to the polarity that was observed for each of the two biasing conditions. The proposed charging mechanism is illustrated in Figs 7 and 8 for the negative and positive bias conditions respectively.

We did not compare results from different irradiation sources, but the similarities noted above between the switch and the accelerometer suggests that the switch might have another property in common with the accelerometer: that a given dose from one type of irradiation (gamma rays versus

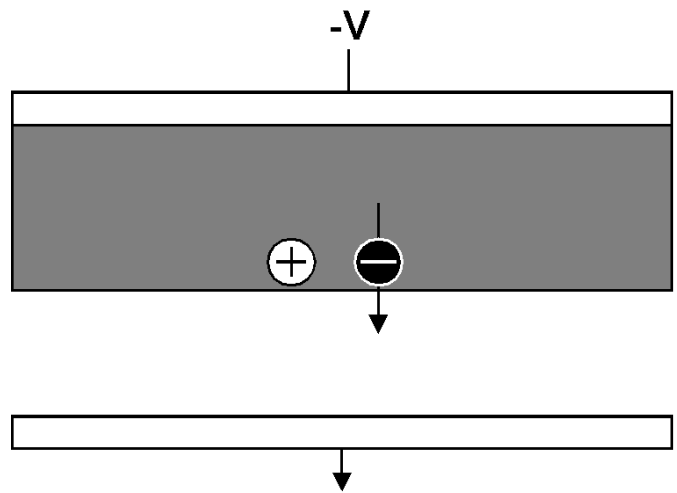


Fig. 7. For negative bias during irradiation, secondary electrons are emitted from the dielectric before becoming thermalized, resulting in a net positive charge at the surface of the dielectric.

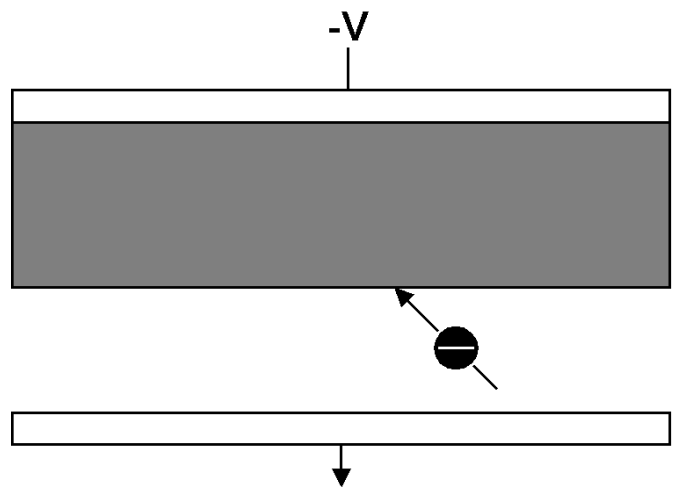


Fig. 8. For positive bias during irradiation, secondary electrons emitted from the lower plate or substrate are attracted to and captured in the dielectric.

protons versus electrons) produces a different response than the same dose from another type of irradiation. If true, then dose alone is not an adequate description of the environment. Additional research is needed to address this issue.

Though it was not directly verified, the lack of significant radiation effects found in previous tests of the HRL Laboratory device could be due to the different dielectric material used. Based on the construction of that device [7] our theory would predict that dielectric charging, were it to persist, would result in a change in the actuation voltage. Since no such effect was noted, it is likely that the dielectric material used has a significantly lower resistivity than the dielectric material used in the devices in this study. However, since test the actuation voltage in the HRL was not directly measured and the bias condition was dynamic rather than static, this conclusion would require further testing.

VII. CONCLUSIONS

As demonstrated in the results presented herein, total dose effects may impact actuation characteristics of MEMS switches, which are operated in moderate total dose environments. The presence of this total dose effect depends on actuator geometry (shown in this work) and actuator materials (suggested by previous work). Of notable significance is the susceptibility of GaAs MEMS devices to radiation effects as found in this work. Such effects, if present, may be eliminated with proper design techniques, as demonstrated in the alternate RSC switch configuration. It is strongly recommended that devices of this type be thoroughly characterized for radiation effects prior to use in systems with a space and/or nuclear radiation environments. It is further recommended that test environments be similar to the application environment.

In this work, a mechanism for creating a charge distribution in the dielectric of the MEMS device is proposed. Further investigations to evaluate this mechanism are proposed and are currently planned in our continuing efforts to evaluate radiation effects in MEMS devices.

VIII. ACKNOWLEDGMENT

The authors would like to thank Thomas George and Joanne Wellman of the Jet Propulsion Laboratory and Ernest Robinson of the Aerospace Corporation for providing the coordination necessary to the success of the tests reported herein.

IX. REFERENCES

- [1] S. Cass, "MEMS in Space," IEEE Spectrum, July 2001.
- [2] J. J. Yao et. Al., "Microelectromechanical system radio frequency switches in a picosatellite mission," Smart Mater. Struct., vol 10, p 1196, 2001.
- [3] A. R. Knudsen et al, "The effects of radiation on MEMS accelerometers," IEEE Trans. Nucl. Sci., vol. 43, no. 6, p. 3122, 1996.
- [4] C. I. Lee et al, "Total dose effects on micromechanical systems (MEMS): accelerometers," IEEE Trans. Nucl. Sci., vol. 43, no. 6, p. 3127, 1996.
- [5] L. P. Schanwald et al, "Radiation effects on surface micromachined comb drives and microengines," IEEE Trans. Nucl. Sci., vol. 45, no. 6, p. 2789, 1998.
- [6] L.D. Edmonds, G.M. Swift, and C.I. Lee, "Radiation Response of a MEMS Accelerometer: An Electrostatic Force", IEEE Trans. Nucl. Sci., vol. 45, pp. 2779-2788, Dec. 1998.
- [7] R.N. Schwartz et al, "Gamma-ray radiation effects on RF MEMS switches," Proceedings of the 2000 IEEE Microelectronics Reliability and Qualification Workshop, October 2000, paper IV.6.
- [8] R.E. Mihailovich et. Al., "MEM Relay for Reconfigurable RF Circuits," Microwave and Wireless Components Letters, vol. 11, no. 2, p. 53, 2001.
- [9] J.R. Reid, "Capacitive switch reliability issues," GOMAC 2002 Digest of Papers, p48, and "Dielectric charging effects on capacitive MEMS actuators," MTT-S 2002 Workshop on Modeling of MEM Switches,